Stability of Human Serum Albumin During Bioprocessing: Denaturation and Aggregation During Processing of Albumin Paste

Jen-Jen Lin,[1] Jeffrey D. Meyer,[1] John F. Carpenter,[1] and Mark C. Manning[2]

Received October 20, 1999; accepted January 10, 2000

Purpose. To assess the impact of various bioprocessing steps on the stability of freshly precipitated human serum albumin (HSA) obtained from pooled human plasma.

Methods. After initial precipitation of HSA from plasma, the resultant paste is either (a) lyophilized or (b) washed with acetone and then air-dried in order to obtain a dry powder. The structure of HSA was examined using Fourier transform infrared (IR) spectroscopy. The extent of aggregation of redissolved HSA was measured using both dynamic light scattering and SDS-polyacrylamide gel electrophoresis (SDS-PAGE).

Results. Both lyophilization and air-drying perturb the secondary structural composition of HSA, as detected by infrared (IR) spectroscopy. Upon dissolution of dried paste, most of the protein refolds to a native-like conformation. However, a small fraction of the protein molecules form soluble aggregates that can be detected by both dynamic light scattering and SDS-PAGE. The level of aggregation is so low that it could not be detected in the bulk by either circular dichroism or IR spectroscopy. The lyophilized protein, which appears to be more unfolded in the solid state than the acetone washed/air-dried material, exhibits a higher level of aggregation upon dissolution.

Conclusions. There is a direct correlation between the extent of unfolding in the solid state and the amount of soluble aggregate present after dissolution. Moreover, the presence of the aggregates persists throughout the remainder of the purification process, which includes dissolution, chromatography, sterile filtration and viral inactivation steps. Analytical methods used to monitor the stability of biopharmaceuticals in the final product can be used to assess damage inflicted during processing of protein pharmaceuticals.

KEY WORDS: albumin; human serum; aggregation; bioprocessing; plasma proteins; infrared spectroscopy.

INTRODUCTION

Most of the research done on stabilizing protein pharmaceuticals has focused on stability in the final container and development of the final formulation (1). By comparison, there has been relatively little published work on the stability of proteins during bioprocessing (2), even though a protein is exposed to a variety of stresses in the manufacturing process, any of which could promote degradation. Most of the work to date has focused on human serum albumin (HSA), particularly with respect to surface adsorption (3,4). In the 1940s, it was discovered that proteins could be precipitated from human plasma by varying the pH and adding ethanol, in what is now known as the Cohn fractionation process (5). By controlling the pH and ethanol content, semi-purified fractions of plasma proteins can be produced. One of the last proteins to precipitate in the Cohn process is human serum albumin (HSA). After precipitation, a wet paste of crude HSA is obtained. Subsequent bioprocessing steps (purification, filtration, pasteurization, etc.) are intended to produce a purified, stabilized form of HSA for commercial use (Fig. 1). In order to obtain a dry, free flowing powder amenable to further purification, the wet HSA paste is either (a) lyophilized or (b) washed with acetone and then air-dried. The effect of each of these treatments on the structure and aggregation state of HSA is examined in this study. Should structural changes occur during the drying of the paste, it is hypothesized that the misfolded protein might be more prone to aggregation upon dissolution or when subjected to any subsequent stresses in the manufacturing process.

In this study, it is shown that the level of aggregate formation correlates with the degree of structural damage that occurs during drying. Furthermore, the soluble aggregates continue to be present throughout the remainder of the purification process, which includes dissolution, chromatographic purification, sterile filtration, and viral inactivation at elevated temperature. The aggregates can be detected even at the penultimate step of the process (sterile filtration immediately prior to heat treatment to inactivate viruses). However, the amount of aggregate present is quite low, and spectroscopic analysis of bulk HSA does not reveal its presence. Only sensitive techniques, such as dynamic light scattering and polyacrylamide gel electrophoresis (PAGE), can detect the presence of these aggregates.

MATERIALS AND METHODS

Materials

Three batches of HSA were obtained from pooled human plasma, designated as lots 1 through 3. All of the lots used in this study had protein concentrations in the final product of 25 % (250 mg/ml). Each lot consisted of a combination of a number of samples or sublots. For example, lot 1 resulted from addition of three different sublots that were acetone washed and air-dried, lot 2 was formed by collection of five different lyophilized sublots, and lot 3 contained three different sublots that were acetone washed and air-dried. Therefore, IR spectra of solid samples were taken of each sublot, in order to demonstrate that each sublot component was similar, and the resultant differences were due to the process and not batch-to-batch variability. Air-dried samples were washed with ten to thirteen volumes of acetone and then allowed to air dry overnight at room temperature. Lyophilized samples were obtained by spreading the paste on trays and lyophilizing until a final water content of less than 10% was obtained. Each process produced a coarse, flowing powder.

Methods

Infrared Spectroscopy

Infrared spectra were obtained with a Nicolet Magna 550 FTIR spectrometer equipped with a DTGS KBr detector. The

[1] Center for Pharmaceutical Biotechnology and Department of Pharmaceutical Sciences, School of Pharmacy, University of Colorado Health Sciences Center, Denver, Colorado 80262.

[2] To whom correspondence should be addressed. (e-mail: mark.manning@uchsc.edu)

0724-8741/00/0400-0391$18.00/0

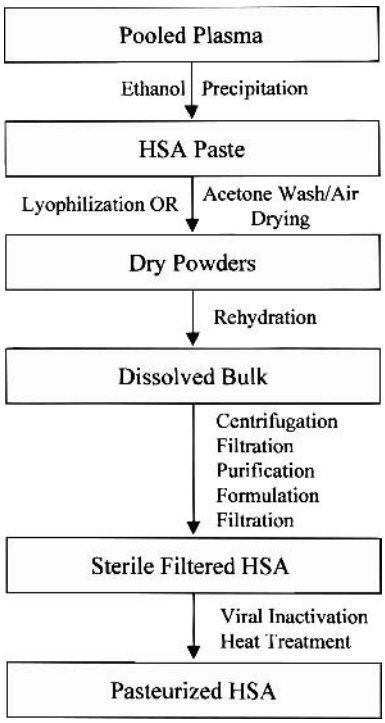

Fig. 1. General scheme for commercial production of HSA.

sample compartment was continually purged with dry air. A total of 256 scans were averaged for each sample. All spectra were recorded at a resolution of 4 cm^{-1} and apodized with the Happ-Genzel function.

Liquid samples were placed in a Wilmad variable pathlength cell, which contains CaF_2 windows, and pathlength was adjusted to approximately 9 μm. Due to the strong absorbance of the water bending mode around 1640 cm^{-1}, a water blank was collected and subsequently subtracted from the absorbance scans, utilizing the Nicolet Omnic software. Correct water subtraction results in a straight baseline between 1800–2300 cm^{-1} (6). Second derivative spectra were calculated utilizing the Nicolet Omnic software. After taking the second derivative, a second derivative water vapor spectrum was subtracted from each sample, with the criteria of obtaining a straight baseline again between 1800–2300 cm^{-1}. Spectra were seven point smoothed and then exported to the Grams software package. Within Grams, the spectra were baseline adjusted, attenuated to the amide I region (1720–1580 cm^{-1}) and the area under each second derivative spectrum was normalized to one (7). The normalized spectra could be compared for area of overlap, as a measure of similarity (7). After normalization, spectra were zero filled to double the number of data points. This means that the number of data points was doubled by extrapolation between the actual values. This makes subsequent processing of the data easier.

Spectra of protein powders were obtained by adding 0.2–0.4 mg of protein to 300 mg of KBr. The protein was gently ground into the KBr with a mortar and pestle, and the powder was then transferred to a die apparatus. The die was placed at approximately 20,000 psi under vacuum for approximately 10 minutes to form a KBr disc. Spectra were collected in the same manner as for liquid samples. Spectral processing was done in exactly the same manner as for water samples, except for the initial liquid water absorbance subtraction step.

Light Scattering Spectroscopy

Light scattering was measured with Dyna Pro-801 dynamic light scattering instrument (Protein Solutions, Charlottesville, VA). Samples were diluted to a concentration of 5 mg/ml, filtered through a Whatman 0.1 μm syringe filter (to remove any dust particles), injected into the sample cell, which was held at a temperature of 25°C. Samples were tested in triplicate, with each reading containing at least 15 independent measurements. The autocorrelation coefficients, and the percentages of light scattering and mass of molecules in each peak of a certain hydrodynamic radius (R_H) were calculated by the software DYNAMICS (Version 2.1). Another program, Dynals (Version 1.12b), was used to calculate the percentages of light scattering for molecules at each of the calculated RH values.

Polyacrylamide Gel Electrophoresis (PAGE) Studies

The gel electrophoresis was run in the Mini-Protein II cell of BioRad. For native gel electrophoresis, 60 μg of each sample was loaded on 3% stacking gel and was separated with 7.5% running gel in tris-glycine electrophoretic buffer (pH 8.6). Constant amperages, 12 mA and 25 mA, were applied for the stacking and separating gels, respectively. For SDS-PAGE, 24 μg samples were heated with or without β-mercaptoethanol before loading on 5% stacking gel with 12% separating gel. Constant voltages, 100 v and 200 v, were applied for stacking and running gels, respectively, in tris-glycine electrophoretic buffer (pH 8.6). Both native and SDS-gels were stained with Coomassie Blue. In order to observe trace amounts of impurities and aggregates, sample wells were intentionally overloaded with HSA solutions.

Circular Dichroism Spectroscopy

The circular dichroism spectra were collected using an Aviv model 62 DS spectropolarimeter (Lakewood, NJ). Samples were diluted to 10 mg/ml and 0.1 mg/ml for collection of near UV and far UV spectra, respectively, and loaded into a strain-free 1 mm pathlength quartz cell. The sample holder was thermostatted at 25°C. Data were collected at 0.5 nm intervals using a 4 second averaging time. The mean residue ellipticity of HSA was calculated using a mean residue weight of 113.6.

RESULTS

Structural Changes Upon Drying and Rehydration

Two different methods for drying wet albumin pastes are commonly in use: shelf lyophilization and acetone washing followed by air drying. The impact of these two drying methods on the structural integrity of HSA is the focus of this study. If HSA is denatured early in the manufacturing process, it may result in an aggregation-competent species that could lead to (i) aggregation immediately upon dissolution or (ii) generation of an unfolded protein species that could act as a seed for more extensive aggregation when the protein is stressed later in the process. Therefore, it is important to assess the overall conformation of HSA at this juncture as well as throughout the manufacturing process.

Small changes in secondary and tertiary structure may account for differences in the propensity of a protein to aggregate (8). Therefore, secondary structural differences between lots of plasma-derived HSA were investigated using IR spectroscopy. Three lots of plasma-derived HSA were examined. Each of them was prepared from mixtures of various sublots of dried albumin samples. These sublots represent different batches of wet albumin paste (cf. Fig. 1) that have either been lyophilized or have been acetone washed and air dried. In the case of lot 1, three sublots of paste were washed with 10 volumes of acetone per kilogram of protein, air dried, and combined. In lot 3, three sublots of albumin paste were acetone washed as well, but with a slightly greater volume of acetone prior to air drying (13 volumes of acetone per kilogram). Each were these lots was air dried overnight. Conversely, lot 2 is comprised of five sublots that have been bulk lyophilized on shelves.

Figure 2 displays second derivative spectra of the amide I band (1700-1600 cm^{-1}) of HSA from each of these sublots of protein powder. For comparison, the IR spectrum of native HSA in aqueous solution is shown. The amide I band arises primarily from the carbonyl stretching vibration and its frequency is dependent on the extent of hydrogen bonding that occurs in different secondary structure types. Therefore, specific frequencies can be correlated with a particular secondary structure (9). In order to resolve these individual components, the second derivative of the absorption band is calculated. In general, the larger the component band, the more of that secondary structure type that occurs in the molecule.

For native HSA, the primary secondary structure in HSA is the α-helix (approximately 60%), which results in a strong band at 1655 cm^{-1} (Fig. 2A). Upon drying, all of the powder samples show deviations from the spectrum of native HSA. In all of the spectra, there is large broadening of the helix band and appearance of new spectra features, especially between 1600 and 1640 cm^{-1}, indicative of increased β-sheet content.

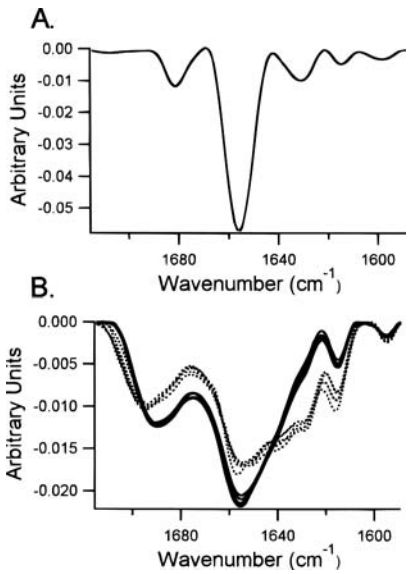

Fig. 2. (A) Second derivative IR spectrum of native HSA in aqueous solution. (B) Second derivative IR spectra of HSA powder samples prepared by acetone washing/air-drying (solid lines) or lyophilization (dashed lines).

In general, the powders that were lyophilized (five sublots eventually incorporated into lot 2) exhibit secondary structure contents that are distinctly less native-like than the acetone-washed/air-dried samples. The α-helix band is diminished in intensity and broadened relative to the acetone-washed samples. Other spectral features, corresponding to β-sheets (1620-1640 cm^{-1}) and β-turns (1660-1685 cm^{-1}) are increased in intensity. These changes indicate that some of the native helical structure of HSA has been converted to loop, turn, and extended strand conformations. Furthermore, broadening of the helix band in both cases indicates perturbation of the native structure. Although visual inspection of the amide I IR spectra indicates that the secondary structure of the lyophilized samples was perturbed to a greater extent, it is possible to quantitate the differences. A method termed area of overlap measures the similarity of two normalized spectra, with a value of 1.0 meaning that the spectra are identical and a value of 0.0 meaning that there is absolutely no similarity (7). Relative to the solution spectrum of native HSA, the average area of overlap for the lyophilized samples was 0.57 while the area of overlap for the acetone-washed/air-dried samples was 0.63. This indicates that the structure is more disrupted when the paste is lyophilized rather than air dried.

Raw absorbance spectra are shown in Fig. 3 for all of the sublots. Narrower bands indicate less structural variability and a more homogeneous conformational population. Note that the width of the amide I envelope is significantly narrower in the acetone-washed samples compared to the lyophilized ones, although both are broader than native HSA. Again, these data are consistent with the description that lyophilized samples contain a broader range of conformations and/or have more structural altered protein than the acetone-washed materials. A greater degree of unfolding in the solid state often correlates with increased tendency to exhibit aggregation upon rehydration and/or exposure to further stress (10).

Despite the extensive structural rearrangement that occurs upon drying, it is known that many proteins refold efficiently during rehydration (11). The question is whether all of the HSA molecules refold properly or whether a small proportion adopts aggregation-competent alternative structures. Based on these findings, one would hypothesize that lot 2, which is comprised of five lyophilized sublots, would be more likely to exhibit soluble aggregates upon rehydration. Therefore, the conformation of HSA after reconstitution was investigated. Upon rehydration of the dried sublots, we refer to these samples as dissolved bulk material.

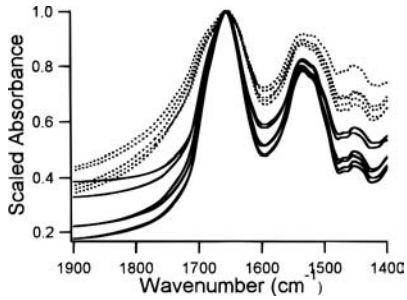

Fig. 3. Absorbance IR spectra of HSA powder samples prepared by acetone washing/air-drying (solid lines) or lyophilization (dashed lines).

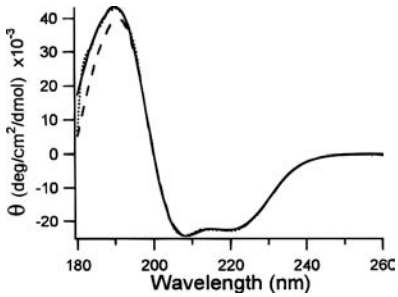

Fig. 4. Far UV CD spectra of dissolved bulk HSA for lot 1 (—), lot 2 (- - -), and lot 3 (····).

Circular dichroism spectroscopy is a powerful tool for assessing changes in both the secondary and tertiary structure of proteins in solution (12). Examination of the far UV ($\lambda \sim$ 180–250 nm) region provides information on the secondary structure composition of a protein. For native HSA, which contains 55–60% α-helix, one would expect to observe negative bands at 222 and 208 nm, a crossover point near 200 nm, and a positive band near 192 nm. Figure 4 shows the far UV CD spectra of lots 1 (acetone-washed/air-dried), 2 (lyophilized), and 3 (acetone-washed/air-dried) for dissolved bulk material. Each of the spectral features noted above are present, indicating that the dominant structure for each dissolved bulk sample is essentially native-like. In other words, the method of drying did not affect the overall structure of rehydrated HSA. Note that there is a slightly lower intensity in the positive band for lot 2, although the crossover point is unaffected. This pattern might suggest that there might be slightly less α-helix content, but, more likely, the noise level for the lot 3 sample was slightly higher, leading to poorer spectral quality at shorter wavelengths, where the signal-to-noise ratio is poorer. Overall, there appears to be little or no secondary structural difference between lots 1, 2, and 3 upon dissolution.

Similar types of comparisons can be made using the near UV region ($\lambda \sim$ 250–350 nm) of the CD spectrum. In this wavelength range, the aromatic side chains give rise to the CD signals. The aromatic signals act as 'reporter' chromophores, sensitive to changes in the local environment around each group. Therefore, any alteration in local tertiary structure and/or aggregation state can cause perturbations of the near UV spectrum. Figure 5 displays the near UV CD spectra for dissolved bulk samples of HSA from lots 1, 2, and 3. The spectra appear as a sloping negative shoulder, with two distinct vibrational fine structure features at 262 and 269 nm. In addition, there is a broad featureless band from 290 to 320 nm. This band can be assigned to disulfides in HSA (12). The signals from 290-260 nm are attributed to tyrosine and phenylalanine. The shape of the spectrum indicates that most of the aromatic side chains lack well defined local environments, with the exception of the residue(s) that give rise to the features at 262 and 269 nm. For the three dissolved bulk samples, little difference is observed in either the secondary or tertiary structural level.

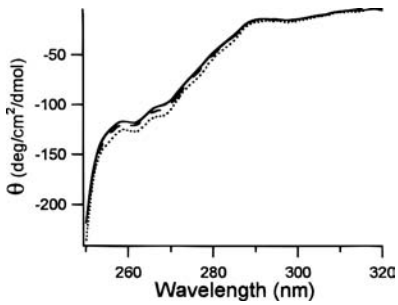

Fig. 5. Near UV CD spectra of dissolved bulk HSA for lot 1 (—), lot 2 (- - -), and lot 3 (····).

Formation of Soluble Aggregates in HSA

While spectroscopic methods examining the dissolved bulk material did not indicate significant differences, there are a number of other analytical techniques that can detect low levels of aggregated protein. The two employed in this study are dynamic light scattering (DLS) and gel electrophoresis. Initial studies on the extent of aggregation in HSA samples were performed using DLS techniques. Plots of DLS data are presented based on light scattering intensity, as well as the total mass of protein involved in aggregate formation. As a larger particle scatters much more light than a small particle (related by r^6), even a very small amount of a large aggregate can be detected. As a result, mass-based plots may appear to be monodisperse for the native species, yet they may exhibit a large amount of scattering from a very small amount of large particles.

Dynamic light scattering intensity can be plotted as a function of hydrodynamic radius (R_H). The monomeric HSA species has a radius near 2–3 nm (20–30 Å), assuming HSA can be modeled as a sphere. Note that there are peaks observed at larger sizes. The inset displays an expansion that indicates that, while lots 1 and 3 (acetone-washed/air-dried) have little, if any, aggregated species, lot 2 (lyophilized) certainly does. These aggregates are calculated to be 30 to 40 nm in radius, all of which remain soluble in aqueous solution. Note that the filter should nominally remove any particles greater than 100 nm across, as a small pore filter (0.1 μm) was used to remove any dust particles. This would allow only smaller, soluble aggregates to pass through. When placed on a mass basis, it is clear that the total amount of soluble aggregate in lot 2 is still quite small (less than 0.1% if one integrates the peak area relative to the monomer), with an average R_H value for the aggregate near 60 nm (Fig. 6).

Presence of Soluble Aggregates Throughout the Purification Process

Dissolved bulk material contains no stabilizing agents and is still far from pure. Therefore, additional bioprocessing steps

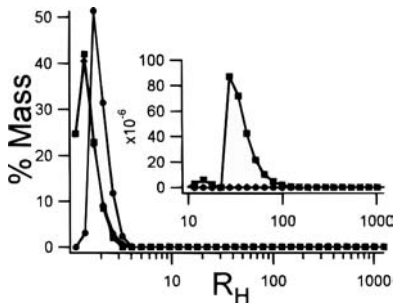

Fig. 6. Plot of mass percent vs. hydrodynamic radius as determined by dynamic light scattering for dissolved bulk samples of lot 1 (●), lot 2 (■), and lot 3 (♦).

have to be taken in order to obtain the final product. After dissolving the bulk material, the protein is filtered, purified, and then formulated with stabilizing agents, such as caprylate and N-acetyl tryptophan. At this point the process is nearly complete, except for the terminal heat treatment step (often called pasteurization) that is intended to inactivate any possible viral contaminant (see Fig. 1). Spectroscopic investigations were conducted on material near the end of the manufacturing process, focusing on pre-pasteurized samples (called 'filtered' or 'sterile filtered') and after the viral inactivation heat treatment ('pasteurized product'). None of these samples displayed any significant differences in secondary structure from each other or from native HSA, based upon the far UV CD spectra (data not shown).

However, these methods are not sensitive to detect the presence of small amounts of structurally altered protein. Therefore, the samples collected immediately prior to heat treatment (sterile filtered samples) and after heating (pasteurized samples) were analyzed by DLS. The mass percent-based plot of the filtered samples indicates that the entire purification process fails to remove the soluble aggregates found in lot 2 (Fig. 7). On the other hand, the purification process does not appear to damage the HSA solution any further either, as the other two acetone-washed lots are relatively free of soluble aggregates. Unlike the pre-pasteurized, filtered samples, all of the lots exhibit some extent of aggregation after heating (at 60° C for ten hours), independent of the method of drying the original paste (data not shown).

In order to verify the DLS results and to discern whether the aggregates are covalently linked, the extent of aggregation in each of these samples was determined using gel electrophoresis. In assessing protein aggregation in HSA, we employed native gels as well as reduced and non-reduced SDS-PAGE gels. Reduced SDS gels were more complicated as there are 17 disulfides in HSA, all of which have different sensitivity to reduction, generating multiple species.

In Fig. 8, representative gel data are presented. The first panel (A) contains the reduced SDS-PAGE data. Increased levels of aggregated protein (see arrow) can be observed in lot 2 (lyophilized) relative to the other two lots (acetone washed/air-dried). The apparent molecular weight would suggest dimers and trimers of HSA are present. The second panel (B) displays the non-reduced gel for lots 1, 2, and 3, as well as two other acetone-washed/air-dried lots (lots 4 and 5). Note that lot 2 again displays a higher level of high molecular weight species (see arrow), independent of the type of gel employed. This finding is consistent with the greater degree of structural damage seen in the powder samples, and is consistent with the dynamic light scattering data. No other lot seems to contain significant amounts of this species.

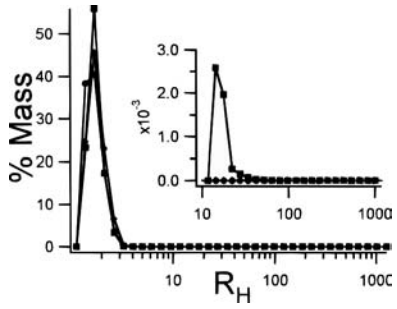

Fig. 7. Plot of mass percent vs. hydrodynamic radius as determined by dynamic light scattering for final filtered bulk samples of lot 1 (●), lot 2 (■), and lot 3 (♦).

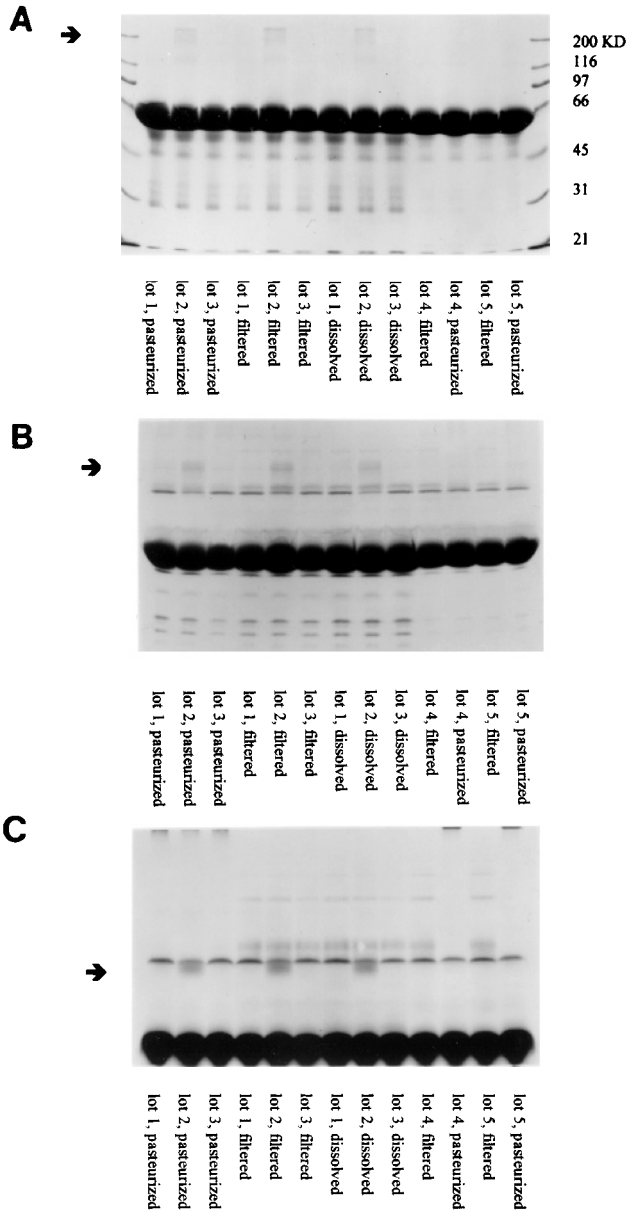

Fig. 8. Polyacrylamide gels of HSA lots. (A) Reduced SDS-PAGE gel. (B) Non-reduced SDS-PAGE gel. (C) Non-denaturing gel.

Panel C displays the native gels for these same samples. Again, there is a significant amount of what appears to an aggregated species in lot 2 (see arrow). In addition, high molecular weight aggregates can be seen at the very top of the gel for all pasteurized samples. This suggests that the aggregates formed during heating are different than those formed during drying of the pastes.

DISCUSSION

Clearly, there are significant effects on the secondary structure of HSA pastes upon drying, with lyophilization appearing

to be more damaging than acetone washing followed by air drying. Unfolding of proteins upon lyophilization is quite common (10). However, it is important to note that the IR spectra are averages and do not indicate whether it is a small amount of protein that is highly unfolded, a large amount of protein that is moderately unfolded, or some combination. Still, lyophilization, as was used with lot 2, does lead to a greater degree of unfolding, and should lead to a greater likelihood of producing an aggregation-competent form of the protein (10,11). In any case, one must remember that the total amount of aggregate present after drying is quite small, sometimes less than 0.1%. This value is determined from DLS, but is verified by the SDS-PAGE data. The filtration associated with sample preparation for DLS measurements might remove some larger aggregates. However, no high molecular weight species could be observed in any of the gels, suggesting the presence of high molecular weight aggregates is minimal.

Upon rehydration in aqueous buffer, the protein appears to refold almost entirely, such that no significant differences could be seen in secondary structure composition as determined by far UV CD spectroscopy. Examination of the near UV CD spectra did not provide any definitive indication that the average tertiary structure was different in dissolved samples from lots 1, 2, and 3. One can conclude that a very large majority of rehydrated HSA is native-like. Given the extent of unfolding in the solid state, one might expect a larger degree of aggregation. However, it appears that HSA is very efficient in refolding after denaturation under these conditions. Note that the polypeptide chain of HSA is constrained by 17 disulfides, so it is not surprising that it is a protein that can refold a large majority of the time.

However, this does not mean that all of the protein refolds properly. Both DLS and gel electrophoresis indicate that lot 2 contains a significant amount of aggregated protein in the dissolved bulk, relative to the other two lots (Figs. 6 and 8). Excision of the bands from the native gels and analysis by SDS-PAGE indicates that they might be comprised of HSA monomers, dimers, and trimers. The only major difference between lot 2 and the other lots is that lot 2 is composed of sublots where the fractionation paste has been lyophilized rather than washed with acetone and air-dried. All of the acetone washed/air-dried lots (lots 4 and 5) show a similar lack of aggregates at the end of the purification process (i.e., at the filtration and pasteurization steps). Since lyophilization leads to a significant disruption of the secondary structure of HSA, as seen by infrared spectroscopy, it appears HSA is another protein where the extent of aggregation can be correlated to the extent of unfolding in the solid state.

Interestingly, the purification and formulation steps fail to remove these aggregated species, as they can be seen in samples just prior to the pasteurization step (Figure 8). Conversely, these steps do not appear to unfold or aggregate the protein either. Once the sample has been subjected to pasteurization, other aggregated species appear in significant amounts (1–3% by weight). These aggregates appear to be different in composition from those arising from lyophilization-induced unfolding, and are currently being investigated.

SUMMARY

This study demonstrates that lyophilization of ethanol-precipitated HSA results in a greater degree of secondary structure perturbation than washing the paste with acetone and air-drying. Upon dissolution, nearly all of the protein refolds to its native conformation, as determined by circular dichroism spectroscopy. However, the lot (number 2) prepared from lyophilized material does display increased levels of soluble aggregate, as detected by both dynamic light scattering and gel electrophoresis. These findings are consistent with earlier work that found that a greater degree of unfolding in the solid state leads to an increased probability of the protein adopting an aggregation-competent structure (8,10).

ACKNOWLEDGMENTS

This work was supported in part by the Colorado Institute for Research in Biotechnology through a graduate fellowship to J.D.M.

REFERENCES

1. W. R. Porter, H. Staack, K. Brandt, and M. C. Manning. Thermal stability of low molecular weight urokinase during heat treatment. I. Effects of protein concentration, pH and ionic strength. *Thrombosis Res.* **71**:265–279 (1993).
2. M. Vrkljan, M. E. Powers, T. M. Foster, J. Henkin, W. R. Porter, J. F. Carpenter, and M. C. Manning. Thermal stability of low molecular weight urokinase during heat treatment. II. Effects of polymeric additives. *Pharm. Res.* **11**:1004–1008 (1994).
3. T. M. Foster, J. J. Dormish, U. Narahari, J. D. Meyer, M. Vrkljan, J. Henkin, W. R. Porter, J. F. Carpenter, and M. C. Manning, Thermal stability of low molecular weight urokinase during heat treatment. III. Effects of salts, sugars, and additional purification. *Int. J. Pharm.* **134**:193–202 (1996).
4. L. Bjerring-Jensen, J. Dam, and B. Teisner. Identification and removal of polymer- and aggregate-forming proteins in human plasma albumin preparations. *Vox Sang* **67**:125–131 (1994).
5. E. J. Cohn, L. E. Strong, W. L. Hughes, Jr., D. J. Mulford, J. N. Ashworth, M. Melin, and H. L. Taylor. Preparation and properties of serum and plasma proteins. IV. A system for the separation into fractions of the proteins and lipoprotein components of biological tissues and fluids. *J. Am. Chem. Soc.* **68**:459–475 (1946).
6. A. Dong and W. S. Caughey. Infrared methods for study of hemoglobin reactions and structures. *Methods Enzymol.*, **232**:139–175 (1994).
7. B. S. Kendrick, A. Dong, S. D. Allison, M. C. Manning, and J. F. Carpenter. Quantitation of area of overlap between second derivative amide I infrared spectra to determine structural similarity of a protein in different states. *J. Pharm. Sci.* **85**:155–158 (1996).
8. J. F. Carpenter, B. S. Kendrick, B. S. Chang, M. C. Manning, and T. W. Randolph. Inhibition of stress-induced aggregation of protein therapeutics. In R. Wetzel (ed.) *Methods in Enzymology*, **309**:236–255 (1999).
9. W. K. Surewicz, H. H. Mantsch, and D. Chapman. Determination of protein secondary structure by Fourier transform infrared spectroscopy: a critical assessment. *Biochemistry* **32**:289–294 (1993).
10. A. Dong, S. J. Prestrelski, S. D. Allison, and J. F. Carpenter. Infrared spectroscopic studies of lyophilization- and temperature-induced aggregation. *J. Pharm. Sci.* **84**:415–424 (1995).
11. S. J. Prestrelski, N. Tedeschi, T. Arakawa, and J. F. Carpenter. Dehydration-induced conformational transitions in proteins and their inhibition by stabilizers. *Biophys. J.* **65**:661–671 (1993).
12. J. F. Towell and M. C. Manning. Circular dichroism in the analysis of protein structure. In N. Purdie and H. G. Brittain (eds.) *Analytical Applications of Circular Dichroism*, Elsevier, 1994, pp. 175–205.